The Astrophysical Journal, 766:74 (9pp), 2013 April 1 doi:10.1088/0004-637X/766/2/74

TRANSPORT OF SOLAR ENERGETIC PARTICLES ACCELERATED BY ICME SHOCKS: REPRODUCING THE RESERVOIR PHENOMENON

G. Qin[1], Y. Wang[1], M. Zhang[2], and S. Dalla[3]
[1] State Key Laboratory of Space Weather, Center for Space Science and Applied Research, Chinese Academy of Sciences, Beijing 100190, China; gqin@spaceweather.ac.cn, ywang@spaceweather.ac.cn
[2] Department of Physics and Space Science, Florida Institute of Technology, Melbourne, FL 32901, USA; mzhang@fit.edu
[3] Jeremiah Horrocks Institute, University of Central Lancashire, Preston, Lancashire PR1 2HE, UK; sdalla@uclan.ac.uk
Received 2012 June 17; accepted 2013 January 28; published 2013 March 11

ABSTRACT

In this work, gradual solar energetic particle (SEP) events observed by multiple spacecraft are investigated with model simulations. Based on a numerical solution of the Fokker–Planck focused transport equation including perpendicular diffusion of particles, we obtained the fluxes of SEPs accelerated by an interplanetary coronal mass ejection driven shock as it propagates outward through the three-dimensional Parker interplanetary magnetic field. The shock is treated as a moving source of energetic particles with an assumed particle distribution function. We look at the time profiles of particle flux as they are observed simultaneously by multiple spacecraft located at different locations. The dependence of particle fluxes on different levels of perpendicular diffusion is determined. The main purpose of our simulation is to reproduce the reservoir phenomenon, during which it is frequently observed that particle fluxes are nearly the same at very different locations in the inner heliosphere, up to 5 AU, during the decay phase of gradual SEP events. The reservoir phenomenon is reproduced in our simulation under a variety of conditions of perpendicular diffusion of particles estimated from the nonlinear guiding center theory (NLGC). As the perpendicular diffusion coefficient increases, the nonuniformity of particle fluxes becomes smaller, making the reservoir phenomenon more prominent. However, if the shock acceleration strength decreases slower than $r^{-2.5}$ with the radial distance r, the reservoir phenomenon might disappear, with limited perpendicular diffusion constrained by the NLGC theory. Therefore, observation of the reservoir phenomenon in gradual SEP events can be used to test qualitatively theories of particle diffusion and shock acceleration.

Key words: Sun: coronal mass ejections (CMEs) – Sun: heliosphere – Sun: magnetic topology – Sun: particle emission

1. INTRODUCTION

Gradual solar energetic particle (SEP) events, usually having high intensity and lasting for several days, are related to the shocks driven by interplanetary coronal mass ejections (ICMEs). In recent years, there have been many gradual SEP events measured by multiple spacecraft that can provide essential information to understand the mechanism of SEP acceleration at the ICME shock and propagation in the interplanetary magnetic field (IMF). Depending on their location, observers in interplanetary space may be connected to different parts of an ICME shock by IMF lines. Simultaneous multi-spacecraft observations in the ecliptic, e.g., by *Helios 1* and *2*, or at different latitudes and radial distances, e.g., by *ACE* and *Ulysses*, usually show the following interesting phenomenon. Although there is a huge difference of particle intensity in the rising phase of SEP time profiles at different positions depending on the magnetic connectivity to the solar event eruption site, during the decay phases, the spatial gradients of SEP fluxes are diminished in all latitudinal, longitudinal, or radial directions, and the SEP fluxes measured by widely separated spacecraft typically present similar intensities within a small ∼2–3 factor (McKibben 1972; McKibben et al. 2001). The phenomenon is called the "reservoir phenomenon" (Roelof et al. 1992) and it has been discussed frequently in many papers (Reames et al. 1997; McKibben et al. 2001; Maclennan et al. 2001; Lario et al. 2003; Tan et al. 2009).

One possible explanation of the SEP reservoir phenomenon is an enhanced perpendicular diffusion (McKibben 1972; McKibben et al. 2001). Several works show that in some events the perpendicular diffusion of energetic particles can be large enough that it should not be neglected compared to the parallel one (e.g., Dwyer et al. 1997; Zhang et al. 2003; Dalla et al. 2003; Wiedenbeck et al. 2010). Theoretical investigations (e.g., Matthaeus et al. 2003) and test particle simulations (e.g., Qin et al. 2002; Qin & Shalchi 2012) found that this can indeed be true. In order to interpret the reservoir phenomenon, Zhang et al. (2009) calculated the transport of SEPs in the three-dimensional Parker IMF from a source fixed near the Sun, and they analyzed the role of perpendicular diffusion. The simulations of Zhang et al. (2009) show that the reservoir phenomenon can be reproduced with perpendicular diffusion. Further studies have also been done on the SEP source location and size effects when considering perpendicular diffusion in SEP transport simulations (He et al. 2011), and in comparison to spacecraft observations (Qin et al. 2011). However, it is noted that the sources of SEPs in Zhang et al. (2009), He et al. (2011), and Qin et al. (2011) are fixed near the solar surface, which is more appropriate for studying higher-energy SEPs. For lower-energy SEPs, however, this is not true because the ICME shock can continuously accelerate particles up to distances of several AU (Cane et al. 1988; Reames 1999).

Unlike the explanation by McKibben (1972), Roelof et al. (1992) and Reames et al. (1997) proposed that ICMEs play an important role in forming reservoirs during the decay phase of an SEP event. They assumed that the magnetic field is twisted by the ICME as it propagates in interplanetary space, which increases the magnetic field magnitude in the sheath region of the ICME. Energetic particles are mirrored by the strong magnetic field (Tan et al. 2009), which prevents the particles from escaping to the outer heliosphere. Therefore, the particles are trapped and can have time to redistribute uniformly throughout the entire heliosphere. In this

explanation, it is assumed that some interplanetary particle transport mechanism is sufficient to eliminate the flux gradient so that perpendicular diffusion is not necessary.

As studied by Kallenrode & Wibberenz (1997) and Kallenrode (2001), the ICME shock can continuously accelerate SEPs as it propagates outward. In their studies (Kallenrode & Wibberenz 1997; Kallenrode 2001), the shock is treated as a moving particle source without considering the perpendicular diffusion of particles, so it is not clear if their calculations can reproduce the reservoir phenomenon. Recently, we calculated the transport of SEPs accelerated by an ICME shock with perpendicular diffusion in the three-dimensional Parker IMF (Wang et al. 2012) where the shock was also treated as a moving source of energetic particles in the same manner as in Kallenrode & Wibberenz (1997). The simulation results in Wang et al. (2012) show that the onset time, peak time, peak intensity, decay rate, and decay duration of ICME shock accelerated SEP fluxes can be significantly influenced by the effect of perpendicular diffusion.

As mentioned above, previous studies explained the reservoir phenomenon to be a result of interplanetary effects (e.g., perpendicular diffusion or magnetic mirroring by ICME). However, it is worth noting that the ICME shock can continuously accelerate low-energy SEPs in interplanetary space. As a result, the radial dependence of shock acceleration might also make important contributions to the reservoir phenomenon, particularly in low-energy SEPs. In this paper, we address the latter problem by extending our previous investigation (Wang et al. 2012) to study the decay phase of ICME-accelerated SEP events by numerically solving the Fokker–Planck focused transport equation. The simulation results can be used to compare with the SEP fluxes observed at different locations so that the physics involved in gradual SEP events can be revealed. In particular, we investigate the roles of perpendicular diffusion and the radial dependence of shock acceleration in the formation of the reservoir phenomenon. In Section 2 we describe our SEP transport model and the model for the ICME shock as a particle source. In Section 3 simulation results are presented. In Section 4 some conclusions based on our simulations are made.

2. MODEL

Our model is based on solving the particle transport equation using the same method as in our previous papers (e.g., Qin et al. 2006; Zhang et al. 2009; Wang et al. 2012). The three-dimensional focused transport equation of SEPs can be written as (Skilling 1971; Schlickeiser 2002; Qin et al. 2006; Zhang et al. 2009; Dröge et al. 2010)

$$\frac{\partial f}{\partial t} = \nabla\cdot(\boldsymbol{\kappa}_\perp\cdot\nabla f) - (v\mu\hat{\boldsymbol{b}} + \boldsymbol{V}^{sw})\cdot\nabla f + \frac{\partial}{\partial\mu}\left(D_{\mu\mu}\frac{\partial f}{\partial\mu}\right) + p\left[\frac{1-\mu^2}{2}(\nabla\cdot\boldsymbol{V}^{sw} - \hat{\boldsymbol{b}}\hat{\boldsymbol{b}}:\nabla\boldsymbol{V}^{sw}) + \mu^2\hat{\boldsymbol{b}}\hat{\boldsymbol{b}}:\nabla\boldsymbol{V}^{sw}\right]\frac{\partial f}{\partial p} - \frac{1-\mu^2}{2}\left[-\frac{v}{L} + \mu(\nabla\cdot\boldsymbol{V}^{sw} - 3\hat{\boldsymbol{b}}\hat{\boldsymbol{b}}:\nabla\boldsymbol{V}^{sw})\right]\frac{\partial f}{\partial\mu}, \quad (1)$$

where $f(\boldsymbol{x}, \mu, p, t)$ is the gyrophase-averaged distribution function; $\boldsymbol{x}$ is the position in a non-rotating heliographic coordinate system; μ, p, and v are the particle pitch-angle cosine, momentum, and speed, respectively, in the solar wind frame; t is the time; $\boldsymbol{V}^{sw} = V^{sw}\hat{\boldsymbol{r}}$ is the solar wind velocity in the radial direction; $\hat{\boldsymbol{b}}$ is a unit vector along the local magnetic field; and L is the magnetic focusing length given by $L = (\hat{\boldsymbol{b}}\cdot\nabla\ln B_0)^{-1}$, with B_0 being the magnitude of the background magnetic field. This equation includes essentially all the important particle transport effects such as particle streaming along a field line, magnetic focusing in the diverging IMF, adiabatic cooling in the expanding solar wind, and the diffusion coefficients parallel and perpendicular to the IMF. The parallel particle mean free path (mfp) $\lambda_\parallel$ is related to the particle pitch-angle diffusion coefficient $D_{\mu\mu}$ as (Jokipii 1966; Earl 1974)

$$\lambda_\parallel = \frac{3v}{8}\int_{-1}^{+1}\frac{(1-\mu^2)^2}{D_{\mu\mu}}d\mu. \quad (2)$$

We use the models of diffusion coefficients following Burger et al. (2008). The pitch-angle diffusion coefficient is adapted from Teufel & Schlickeriser (2003):

$$D_{\mu\mu}(\mu) = \left(\frac{\delta B_{\rm slab}}{B_0}\right)^2\frac{\pi(s-1)}{4s}k_{\rm min}vR^{s-2}(\mu^{s-1}+h)(1-\mu^2), \quad (3)$$

where $\delta B_{\rm slab}$ is the magnitude of the slab component of the turbulence, s is the spectral index in the inertial ranges, $k_{\rm min}$ is the lower limit of the wave number of the inertial range in the slab turbulence power spectrum, $R = pc/(|q|B_0)$ is the particle Larmor radius, and q is the particle charge. h comes from the nonlinear effect of magnetic turbulence on the pitch-angle diffusion at 90° particle pitch angle or $\mu = 0$ (Beeck & Wibberenz 1986; Qin & Shalchi 2009). In our simulations, we set $s = 5/3$, $k_{\rm min} = 1/l_{\rm slab} = 33\ {\rm AU}^{-1}$, and $h = 0.01$, where $l_{\rm slab}$ is the slab turbulence correlation length. $\delta B_{\rm slab}$ is assumed to be proportional to the magnitude of the local background magnetic field with the ratio of their power $(\delta B_{\rm slab})^2/(B_0)^2 = A$. Different parallel particle mean free path values could be obtained by altering the ratio A. A large A represents a condition of a high level of magnetic turbulence. It is noted that for lower-energy SEP transport in the inner heliosphere, the drift effects can be neglected.

The perpendicular diffusion coefficient is taken from the nonlinear guiding center (NLGC) theory (Matthaeus et al. 2003) with the following analytical approximation (Shalchi et al. 2004, 2010):

$$\boldsymbol{\kappa}_\perp = \frac{1}{3}v\left[\left(\frac{\delta B_{\rm 2D}}{B_0}\right)^2\sqrt{3\pi}\frac{s-1}{2s}\frac{\Gamma\left(\frac{s}{2}+1\right)}{\Gamma\left(\frac{s}{2}+\frac{1}{2}\right)}l_{\rm 2D}\right]^{2/3} \times\lambda_\parallel{}^{1/3}(\mathbf{I} - \hat{\mathbf{b}}\hat{\mathbf{b}}), \quad (4)$$

where $B_{\rm 2D}$ and $l_{\rm 2D}$ are the magnitude and the correlation length of the 2D component of magnetic turbulence, respectively. Γ is the gamma function. Here, for simplicity, $\boldsymbol{\kappa}_\perp$ is set to be independent of μ, since particle pitch-angle diffusion is usually much faster than perpendicular diffusion, so before perpendicular diffusion takes effect, the particles have already sampled the entire range of pitch angles. $\mathbf{I}$ is a unit tensor. In our simulations, we set $(\delta B_{\rm slab})^2/(\delta B_{\rm 2D})^2 = 0.25$ (Bieber et al. 1994), $s = 5/3$, and $l_{\rm 2D} = 3\times10^{-3}$ AU. Because $(\delta B_{\rm slab})^2 = A(B_0)^2$, we get $(\delta B_{\rm 2D})^2 = 4A(B_0)^2$. As a result, the mean free path of parallel and perpendicular diffusion can be altered simultaneously by changing the ratio A. Alternatively, the analytical approximation for NLGC theory by Zank et al. (2004) could also be used in this work.

In our model, we need a boundary condition at the ICME shock that is the source of particle injection. Since the theory of

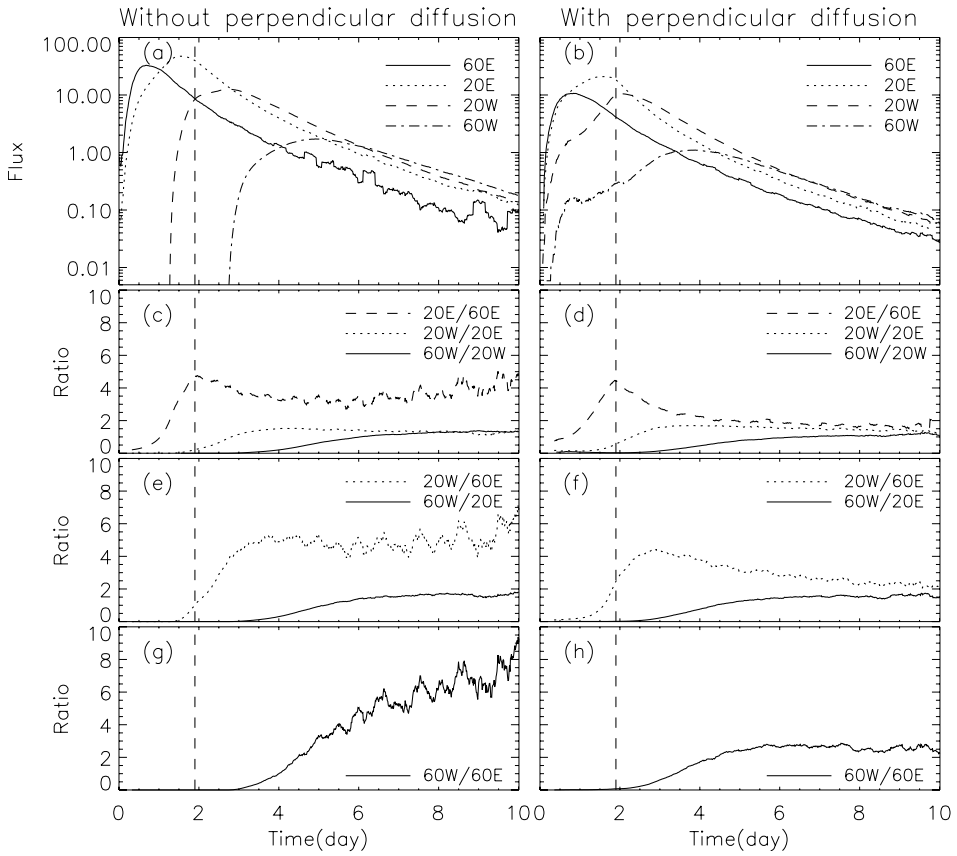

Figure 1. Comparison of 5 MeV proton fluxes with perpendicular diffusion (right panels) and without perpendicular diffusion (left panels). The observers are located at 1 AU in the ecliptic, but at different longitudes. The two top panels show fluxes, and the rest of the panels show flux ratios. The vertical dashed lines indicate the shock passage at 1 AU.

particle injection and shock acceleration is not reliable enough, we choose to specify the distribution of accelerated particles at the boundary with an assumed dependence on particle energy and source location. The assumed source particle distribution at the shock approximately includes all the effects of particle injection and acceleration by the ICME shock (Wang et al. 2012). As the shock propagates outward, we use a series of partial spherical onion shells to model the region swept by the shock. This propagating shock injection model is similar to that in Zank et al. (2000). We neglect the effect of strong scattering by enhanced waves in the vicinity of the shock. Since we study relatively high-energy protons (5 MeV), we assume that particles are not re-accelerated by the shock after they are released. The ICME shock is assumed to propagate only in the radial direction without lateral expansion. The shock nose is in a radial line passing through the center of the partial onion shells. When an observer is connected to the shock by an IMF line, the intersection of the field line on the shock is called the cobpoint (Heras et al. 1995). The cobpoint moves along the shock front toward the east as the shock propagates outward. The source of SEP injection from the shock is modeled by a boundary value $f_b(r, \theta, \varphi, p, t)$ (Kallenrode & Wibberenz 1997; Kallenrode 2001; Wang et al. 2012),

$$f_b = a\delta(r - v_s t)\left(\frac{r}{r_c}\right)^{\alpha(p)} \exp\left[-\frac{|\phi(\theta,\varphi)|}{\phi_c(p)}\right] \times p^{-\gamma} H(\phi_s - |\phi(\theta,\varphi)|), \quad (5)$$

where γ is the shock injection power-law spectrum index, isotropic particles are injected from the shock at a solar distance $r = r_0 + r_s$ with inner boundary r_0, the solar distance unit $r_c = 1$ AU, $\alpha(p)$ is a power-law index that measures the particle injection rate as a function of radial distance, $\phi(\theta, \varphi)$ is the angle between the shock nose and any point (θ, φ) on the shock front where the particles are injected, ϕ_c describes how fast the shock injection decreases toward the flanks of the shock, and $H(x)$ is the Heaviside step function, with ϕ_s being the half angular width of the shock. For a detailed description of the shock model in our simulations, please refer to Wang et al. (2012).

Table 1
Model Parameters Used in the Calculations

Parameter	Physical Meaning	Value
V^{sw}	Solar wind speed	400 km s^{-1}
v_s	Shock speed	870 km s^{-1}
γ	Shock injection spectrum index	5
E	Particles energy	5 MeV
r_{b0}	Inner boundary	0.05 AU
r_{b1}	Outer boundary	50 AU
r_c	Solar distance unit	1 AU

In the simulations, the SEP transport equation (1) is solved by a time-backward Markov stochastic process method (Zhang 1999; Qin et al. 2006).

3. RESULTS

Table 1 shows the parameters used in this paper unless otherwise stated in the text. Note that we use a Parker field model for the IMF, and the twisted magnetic field and strong

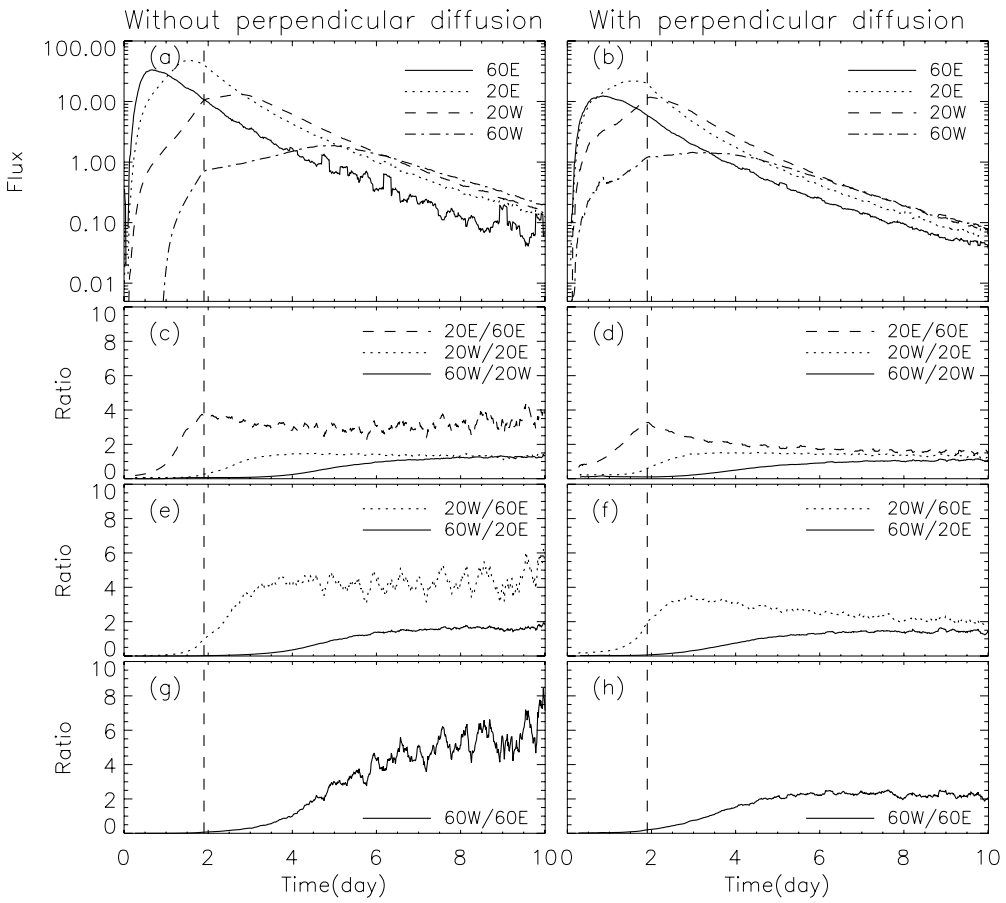

Figure 2. Similar to Figure 1 but with a shock half-width $\phi_s = 90°$.

scattering near the ICME shock are not included. As a result, the shock spikes are absent in our simulation results. In addition, the mean free paths of the parallel and perpendicular diffusion are altered simultaneously by changing the ratio A.

3.1. In the Ecliptic

Figure 1 shows our simulation results of the omnidirectional flux for 5 MeV protons detected at four locations at 1 AU in the ecliptic and longitude, 60W, 20W, 20E, and 60E. The longitude of the observer is measured relative to the shock nose direction. The label "20E/60E" indicates the ratio of the flux detected at 20E to that at 60E. The observers' positions relative to the shock nose direction are similarly named in the rest of the paper. In Figure 1 the vertical dashed lines indicate the shock passage at 1 AU. In the cases with perpendicular diffusion, we set ratio $A = 1.5, \lambda_\parallel = 0.13$ AU, $\lambda_\perp = 0.009$ AU (giving $\lambda_\perp/\lambda_\parallel = 0.07$) at 1 AU. In the cases without perpendicular diffusion, we set ratio $A = 1.5$, $\lambda_\parallel = 0.13$ AU, $\lambda_\perp = 0$ AU. The half-width of the shock ϕ_s is set to 35°. According to the results of comparison between observations and simulations (Kallenrode 1997), typical parameters related to the shock injection rate in Equation (5) are $\alpha = -2.5$ and $\phi_c = 15°$. Note that the relatively higher turbulence level A we choose could be considered the solar maximum condition.

In Figure 1, the left panels ((a), (c), (e), and (g)) and the right ones ((b), (d), (f), and (h)) correspond to the cases without and with perpendicular diffusion, respectively. The top panels ((a) and (b)) labeled "Flux" on the y-axis show the time variation of the omnidirectional fluxes detected at the four different locations, and the remaining panels with the y-axis labeled "Ratio" show the ratios of fluxes between any two locations. If the flux ratio in the decay phase detected by two observers at different positions is smaller than a threshold value, which we set to a value of 3, the fluxes are considered similar enough and the reservoir phenomenon is obtained (note that we always choose to divide the larger flux by the smaller flux during the decay phase to make the ratio larger than 1). The first row of "Ratio" panels (c) and (d), the second row of "Ratio" panels (e) and (f), and the bottom panels (g) and (h) show the flux ratios between observers separated by 40°, 80°, and 120°, respectively. From panels (d), (f), and (h), it is shown that with perpendicular diffusion all the flux ratios are smaller than the threshold value 3 in the decay phases. However, from panels (c), (e), and (g), it is shown that without perpendicular diffusion the flux ratios vary more significantly with the separation between the observers and their positions relative to the shock nose (east or west side). From panel (c) we can see that without perpendicular diffusion and for small separation, 40°, between the observers, the flux ratios are smaller than 3 when the observers are located near the shock nose, i.e., "20W/20E," or to the west of the shock nose, i.e., "60W/20W," but the flux ratio is not smaller than 3 when the observers are located to the east of the shock nose, i.e., "20E/60E." Furthermore, as the separation of the observers becomes larger, i.e., 80°, in panel (e), the flux ratios are larger relative to the ones with smaller separation, and the ratio is larger than 3 when one of the observers is located in the far east, i.e., "20W/60E," but the ratio is still smaller than 3 when all the observers are not located in the far east, i.e., "60W/20E." In panel (g), the flux ratios are even larger when the separation of

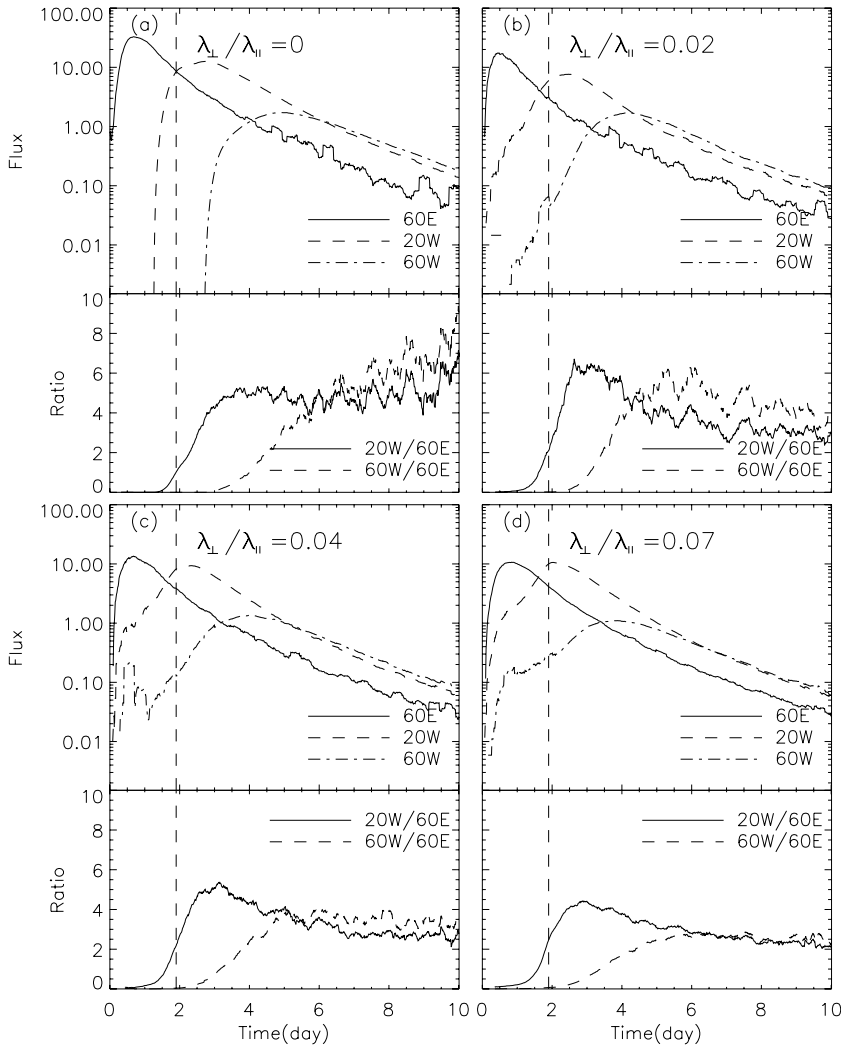

Figure 3. Comparison of 5 MeV proton fluxes seen by observers in the ecliptic at different longitudes and mean free path: (a) $\lambda_\perp/\lambda_\parallel = 0$; (b) $\lambda_\perp/\lambda_\parallel = 0.02$; (c) $\lambda_\perp/\lambda_\parallel = 0.04$; and (d) $\lambda_\perp/\lambda_\parallel = 0.07$. The vertical dashed lines indicate the shock passage at 1 AU.

the observers increases to 120°, i.e., "60W/60E." In the ecliptic, the field lines of different observers are connected to different parts of the shock front. Due to the variation of shock injection strength as a function of the radial distance and longitude, the time profile of flux is very sensitive to the injection strength at the cobpoints (Wang et al. 2012). In the decay phase, the cobpoints of the observers in the far east (e.g., 60E) have moved far away to the eastern side of the shock and their shock injection strength is very small compared to that of other observers at 60W. Therefore, observers in the east have a larger longitudinal gradient without perpendicular diffusion.

From Figure 1 we can see that without perpendicular diffusion, the reservoir phenomenon can only be obtained when all of the observers are not located on the far east side of the shock and their separation is not very large. But with perpendicular diffusion, the reservoir phenomenon can be obtained for all the cases we studied, even when the observers are located on the far east side of the shock nose or they are separated by large longitudinal distance.

It might be argued that without perpendicular diffusion the reservoir phenomenon cannot be obtained for the cases "20W/60E" and "60W/60E" in Figure 1 because the shock half-width, which we set to be $\phi_s = 35°$, is too small. In Figure 2 we show the results of simulations similar to the cases in Figure 1, with the only difference that the shock half-width is now $\phi_s = 90°$. From the figure we can see that even with a much wider 90° shock half-width, the reservoir phenomenon still cannot be obtained in "20W/60E" and "60W/60E" without perpendicular diffusion. However, with perpendicular diffusion the reservoir phenomenon can be obtained.

Next, we investigate the influence of the perpendicular diffusion strength on the longitudinal variation of SEP fluxes. In Figure 3, the input parameters of simulations are similar to the cases in Figure 1, with the only difference being the parallel and perpendicular mean free paths. Three observers are located at 1 AU in the ecliptic with different longitudes, 60E, 20W, and 60W. From panels (a) to (d), the perpendicular mean free path $\lambda_\perp$ at 1 AU of the 5 MeV particles is changed from 0, 0.006, 0.008, to 0.009 AU, with the parallel mean free path at 1 AU varying from 0.13, 0.34, 0.19 to 0.13 AU. In panel (a), without perpendicular diffusion, the flux ratio is always larger than 3 in the decay phase, so the reservoir phenomenon is not obtained. As the perpendicular diffusion increases from panels (b) to (d), the flux ratio in the decay phase becomes increasingly smaller. In particular, in panel (d), the perpendicular mean free path of the 5 MeV protons at 1 AU is 0.009 AU, or 0.07 of the parallel one; the flux ratios are smaller than 3 in the decay phase, so the reservoir phenomenon is reproduced.

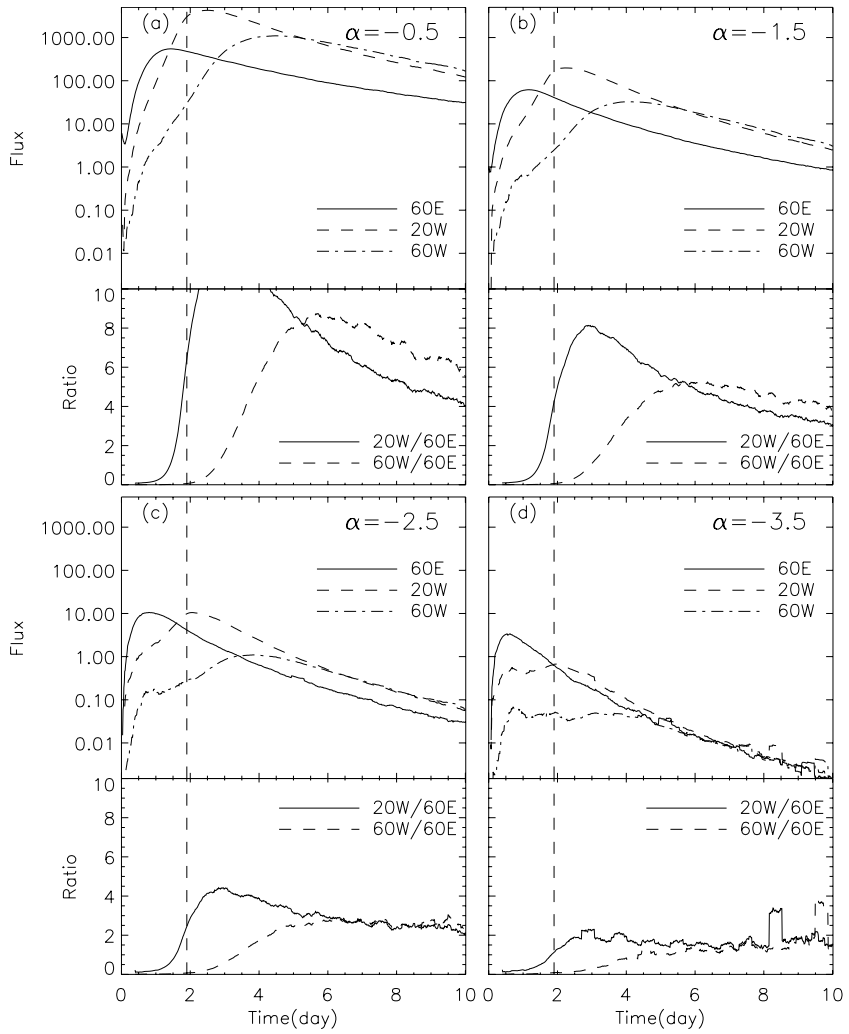

Figure 4. Comparison of 5 MeV proton fluxes seen by observers in the ecliptic with different radial dependences of shock injection and acceleration strength: (a) $\alpha = -0.5$; (b) $\alpha = -1.5$; (c) $\alpha = -2.5$; and (d) $\alpha = -3.5$. The vertical dashed lines indicate the shock passage at 1 AU.

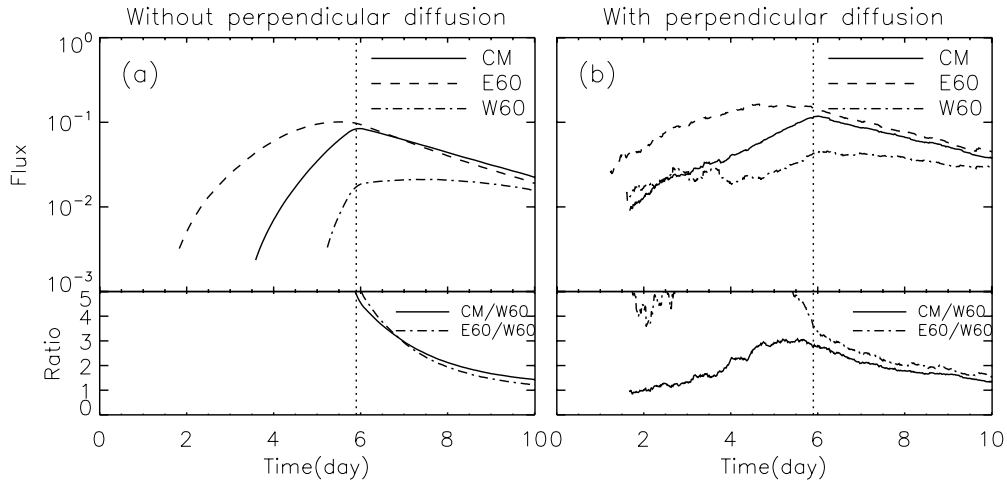

Figure 5. Comparison of 5 MeV proton fluxes at high latitude (60N) with and without perpendicular diffusion. The vertical dotted lines indicate the shock passage at 3 AU. The "CM" in the figure means center meridian.

In Figure 4, we show the results of simulations with different values of power-law index α for the shock injection and acceleration strength as a function of radial distance. The parameter α changes from $-0.5, -1.5, -2.5$, to -3.5. The shock injection and acceleration strength decreases more quickly with a smaller α as the shock propagates in the interplanetary space. We set $\lambda_{\parallel} = 0.13$ AU and $\lambda_{\perp} = 0.009$ AU in the four panels, which are the same as in panel (d) of Figure 3. In panels (a) and (b), the reservoir phenomenon is not obtained. As α decreases from (a) to (d), the flux ratios in the decay phase

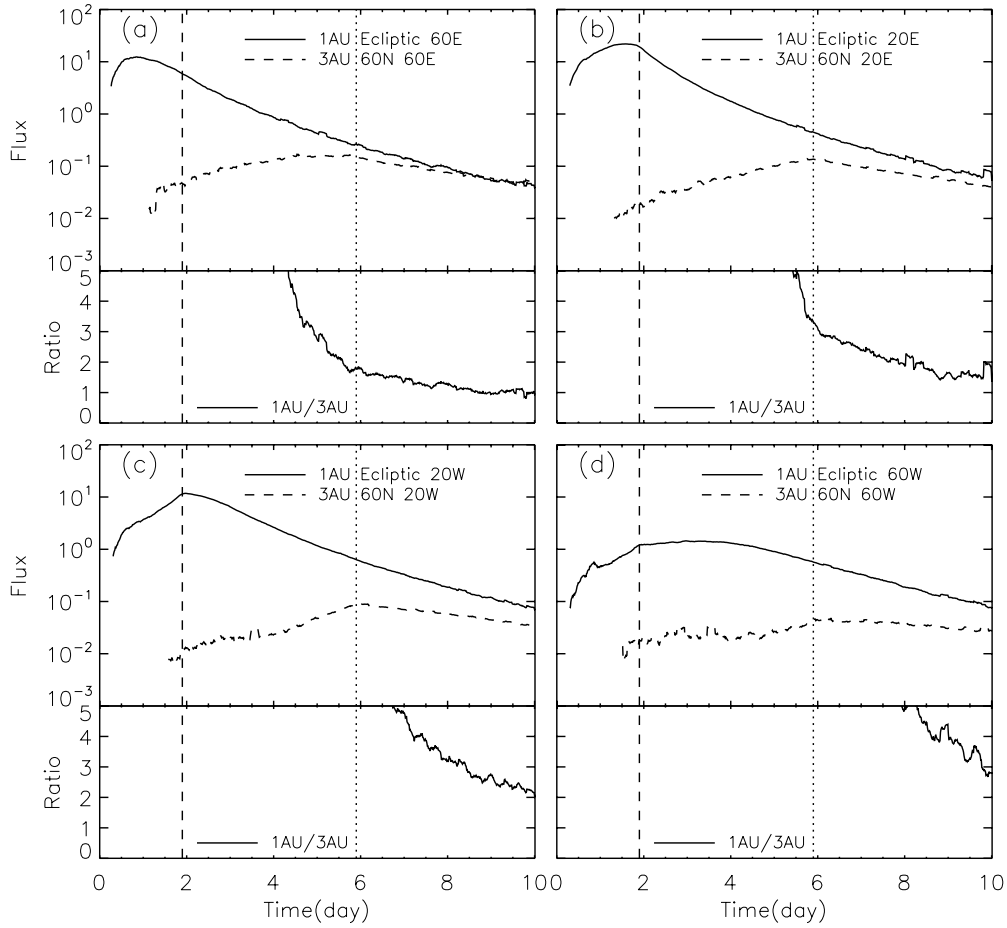

Figure 6. Comparison of 5 MeV proton fluxes with perpendicular diffusion between observers at 1 AU in the ecliptic and at 3 AU, 60N high latitude. The longitudes of the two observers are (a) 60E, (b) 20E, (c) 20W, and (d) 60W. The vertical dashed and dotted lines indicate the shock passage at 1 AU and 3 AU, respectively.

become increasingly smaller. In panels (c) and (d), the reservoir phenomenon is reproduced in the decay phase. We find that the quicker the shock acceleration strength decreases with radial distance, the more easily the reservoir phenomenon can be established. There are two factors leading to this result: (1) the cobpoints of the three observers are closer to each other when the shock is near the Sun, so the difference in the injection strengths between the three observers is smaller than at later times when the shock has propagated outward and (2) a quicker decrease of the shock injection and acceleration strength makes the decay phase appear earlier, so that perpendicular diffusion has more time to erase the gradient in the fluxes between the observers. The density of the seed particles that are injected into the shock for acceleration is proportional to the solar wind density, which varies with the radial distance as r^{-2}. Furthermore, the upstream Mach number increases as the ICME shock propagates outward due to adiabatic cooling, which makes it more difficult to inject the seed particles into the shock acceleration. Magnetic field strength and its turbulence level also decrease rapidly with the radial distance, making shock particle acceleration slower. All of these factors indicate that the α index is usually less than -2, and thus the formation of the SEP reservoir phenomenon is more likely when the perpendicular diffusion is large enough.

3.2. At High Latitudes

Figure 5 shows simulation results for observers located at 60N and 3 AU with several different longitudes in the cases with and without perpendicular diffusion. The half-width of the shock ϕ_s is 90°. We set $\lambda_\parallel = 0.13$ AU and $\lambda_\perp = 0$ AU in panel (a), and $\lambda_\parallel = 0.13$ AU and $\lambda_\perp = 0.009$ AU in panel (b). The vertical dotted lines indicate the shock passage at 3 AU. The label "CM" in this figure means center meridian.

In Figure 5, the flux ratios in the decay phases are all much smaller than the threshold value of 3. In fact, the ratios are smaller than 2 most of the time. In panel (b), the onset time of the fluxes is earlier than in panel (a). Compared with the flux ratios at the observers in the ecliptic shown in Figure 1, we find that the flux ratios in the decay phase are smaller in Figure 5 when the observers are at high latitude 60N. In the ecliptic, the change of the particle injection strength at the cobpoints is larger and can cause more significant difference in fluxes at different longitudes. However, at high latitude 60N, the variation of the shock acceleration strength is smaller than in the ecliptic for the same longitude range. As a result, the difference of the fluxes in the decay phases at different longitudes becomes smaller.

Next, in Figure 6 we look at the simulation results for observers located at different latitudes with perpendicular diffusion. The input parameters are the same as in Figure 5. In each of panels (a), (b), (c), and (d), we compare fluxes at the position of two observers, one at 1 AU in the ecliptic and the other at 3 AU 60N latitude. $r = 3$ AU is chosen for the comparison of our simulation results with *Ulysses* observations. The dashed and dotted lines indicate the shock passage at 1 and 3 AU, respectively. In Figure 6, the flux is larger at the observer at 1 AU in the ecliptic, since the shock acceleration strength is larger at the closer radial distance in the ecliptic than that at 3 AU high

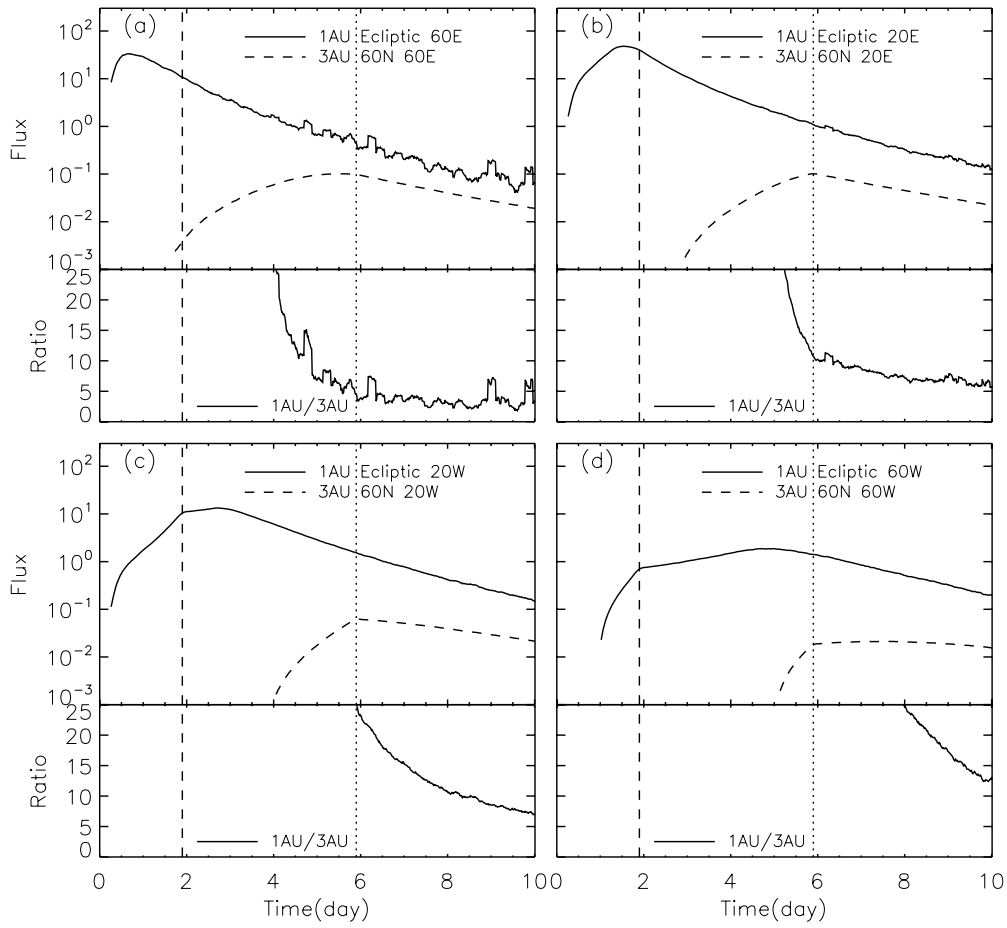

Figure 7. Similar to Figure 6 but without perpendicular diffusion.

latitude 60N. The observer's field line is connected to the shock earlier in the ecliptic. For all the cases with observers located in 60E, 20E, 20W, and 60W, in panels (a), (b), (c), and (d), respectively, the fluxes seen by the observers in the ecliptic have sharper peaks than those of high latitude ones because the shock injection strength at the cobpoints changes more significantly at 1 AU in the ecliptic. In addition, the flux peaks detected by the observers in the ecliptic are much larger than those detected by observers at high latitude. However, during the decay phases after the flux peaks, the difference between the fluxes detected by observers with different latitudes becomes small, and the flux ratios are smaller than 3, so the reservoir phenomenon is reproduced.

In Figure 7, the simulations are similar to that in Figure 6; the only difference is that perpendicular diffusion is not included in Figure 7. We see that the reservoir phenomenon is absent in panels (b)–(d). The reservoir phenomenon occurs only in panel (a). In panels (b)–(d), the flux ratios are all larger than 5. Therefore, the results in Figure 7 suggest that perpendicular diffusion is very important in the establishment of the reservoir phenomenon at different latitudes.

4. CONCLUSIONS

In this paper, we have studied the effect of perpendicular diffusion on the transport of 5 MeV protons accelerated by interplanetary shocks which propagate outward in three-dimensional Parker IMF. In our model, we assume an ICME shock as a moving source of SEPs with some varying injection strengths as a function of space and time. Our model is based on a Fokker–Planck particle transport equation that includes many important particle transport effects, such as particle streaming along field line, magnetic focusing in a diverging IMF, adiabatic deceleration in an expanding solar wind, and diffusion parallel and perpendicular to the IMF. By numerically solving the Fokker–Planck equation of energetic particles, we have investigated the fluxes when the observers are located at different latitudes, longitudes, and radial distances. The following are the major results of our paper.

The reservoir phenomenon was previously assumed to be caused by interplanetary effects (e.g., perpendicular diffusion or disturbances produced by ICME). We found that, in order to reproduce the SEP reservoir phenomenon, aside from interplanetary modulation, the particle injection must take place mainly close to the Sun. Both of these establish the importance of the perpendicular diffusion of particles: (1) the with majority of particles injected early in the SEP event, perpendicular diffusion can have more time to be effective; (2) with a larger perpendicular diffusion, the SEP reservoir phenomenon will be more likely to occur.

With perpendicular diffusion, the energetic particles moving in interplanetary space can cross the average IMF lines. In our simulations, according to the results of the comparison between observations and simulations (Kallenrode 1997), we set the shock injection strength parameters $\alpha = -2.5$ and $\phi_c = 15^\circ$ to be the "typical" shock. We find that with a strong enough perpendicular diffusion (e.g., $\lambda_\parallel = 0.13$ AU and $\lambda_\perp = 0.009$ AU at 1 AU), we can efficiently diminish all latitudinal, longitudinal,

and radial gradients of fluxes, with the ratios of fluxes at any two locations reduced to below 3 in the decay phase, thus reproducing the reservoir phenomenon. In the cases of $\alpha = -0.5$ and $\alpha = -1.5$, the reservoir phenomenon disappears in some simulation results. But in the case of $\alpha = -3.5$, the ratios in the decay phase of fluxes are smaller than the "typical" shock with $\alpha = -2.5$. With a smaller α, the difference in the injection of particles among different observers is smaller, so it is easier to reproduce the reservoir phenomenon. As a result, the reservoir phenomena are controlled by the combined effects of perpendicular diffusion and particle injection strength as a function of radial distance.

When observers are located in the ecliptic, different observers' field lines can connect to different parts of the shock front. Since the shock injection strength changes with radial distance and longitudinal angle, the time profiles of fluxes are sensitive to the shock injection strength at the cobpoints. As a result, the location of an observer has a great effect on the time profiles of fluxes. In addition, the flux peak arrives earlier when the observer is located at the eastern flank of the shock, and the flux peak arrives later when the observer is located at the west. Without perpendicular diffusion, the reservoir phenomenon can be reproduced when the observers are located very closely except at the far east of the shock nose. When the observers are located far away from each other, or one of them is to the far east of the shock nose, the difference of fluxes in the decay phases between observers can be very large. Since in the decay phase the cobpoints of far east observers are near the far shock flanks and disconnect from the shock front very early, the eastern observers can have a larger longitudinal gradient without perpendicular diffusion. However, with a strong enough perpendicular diffusion, the difference of fluxes in the decay phases could be reduced to a small enough value, so that the reservoir phenomenon is reproduced.

When observers are located at high latitude (e.g., 60N), the shock acceleration strengths at the cobpoints are smaller than in the ecliptic. Because the number of injected particles are smaller at high latitude, the gradients of fluxes at different cobpoints in the decay phases are much smaller than in the ecliptic. Therefore, it is easier to reproduce the reservoir phenomenon with perpendicular diffusion when observers are located at high latitudes.

In addition, when one observer is located in the ecliptic, and the other is located at high latitude 60N, the reservoir phenomenon can be reproduced with perpendicular diffusion. However, without perpendicular diffusion, the reservoir phenomenon can only be reproduced when the flux deceases very quickly in the case of 60E.

In our model, we use a set of typical parameters in Table 1 to simulate SEP transport. We ignore the disturbance of the IMF caused by shock or ICME for the simplicity. In principle, the disturbance in the magnetic field can help the particles redistribute in space. If the disturbance is included in our model, the level of perpendicular diffusion needed to reproduce the reservoir phenomenon could be further reduced, so that the ratio of the perpendicular diffusion to the parallel one might be less than 0.07, the value used in this paper. It is also noted that the basic difference between this simulation and the one in Zhang et al. (2009) for the reservoir phenomenon is that this time we have an SEP source that is continuously injected into the moving shock front, while the previous simulation had a fixed source near the Sun. This simulation is more appropriate for low-energy particles, whereas previous simulations were made for high energies. In future work, we intend to include a realistic three-dimensional ICME shock, so that the SEP acceleration and transport in the heliosphere can be investigated more precisely.

We are partly supported by grants NNSFC 41125016, NNSFC 41074125, the CMA grant GYHY201106011, and the Specialized Research Fund for State Key Laboratories of China. The computations were performed by Numerical Forecast Modeling R&D and the VR System of the State Key Laboratory of Space Weather and the Special HPC work stand of the Chinese Meridian Project. M.Z. was supported in part by the NSF under grant AGS-1156056 and by NASA under grant NNX08AP91G. S.D. acknowledges funding from the European Union Seventh Framework Programme (FP7/2007-2013) under grant agreement No. 263252 [COMESEP].

REFERENCES

Beeck, J., & Wibberenz, G. 1986, ApJ, 311, 437
Bieber, J. W., Matthaeus, W. H., Smith, C. W., et al. 1994, ApJ, 420, 294
Burger, R. A., Krüger, T. P. J., Hitge, M., & Engelbrecht, N. E. 2008, ApJ, 674, 511
Cane, H., Reames, D., & Von Rosenvinge, T. 1988, JGR, 93, 9555
Dalla, S., Balogh, A., Krucker, S., et al. 2003, GeoRL, 30, 8035
Dröge, W., Kartavykh, Y. Y., Klecker, B., & Kovaltsov, G. A. 2010, ApJ, 709, 912
Dwyer, J. R., Mason, G. M., Mazur, J. E., et al. 1997, ApJL, 490, L115
Earl, J. A. 1974, ApJ, 193, 231
He, H.-Q., Qin, G., & Zhang, M. 2011, ApJ, 734, 74
Heras, A. M., Sanahuja, B., Lario, D., et al. 1995, ApJ, 445, 497
Jokipii, J. R. 1966, ApJ, 146, 480
Kallenrode, M. 1997, JGR, 102, 22347
Kallenrode, M. 2001, JGR, 106, 24989
Kallenrode, M., & Wibberenz, G. 1997, JGR, 102, 22311
Lario, D., Roelof, E. C., Decker, R. B., & Reisenfeld, D. B. 2003, AdSpR, 32, 579
Maclennan, C. G., Lanzerotti, L. J., & Hawkins, S. E., III. 2001, in Proc. 27th Int. Cosmic Ray Conf., ed. W. Droege, H. Kunow, & M. Scholerin (Princeton, NJ: Rinton)
Matthaeus, W. H., Qin, G., Bieber, J. W., & Zank, G. P. 2003, ApJL, 590, L53
McKibben, R. B. 1972, JGR, 77, 3957
McKibben, R. B., Connell, J. J., Lopate, C., et al. 2001, in Proc. 27th Int. Cosmic Ray Conf., ed. W. Droege, H. Kunow, & M. Scholerin (Princeton, NJ: Rinton)
Qin, G., He, H.-Q., & Zhang, M. 2011, ApJ, 738, 28
Qin, G., Matthaeus, W. H., & Bieber, J. W. 2002, ApJ, 578, L117
Qin, G., & Shalchi, A. 2009, ApJ, 707, 61
Qin, G., & Shalchi, A. 2012, AdSpR, 49, 1643
Qin, G., Zhang, M., & Dwyer, J. R. 2006, JGR, 111, A08101
Reames, D. 1999, SSRv, 90, 413
Reames, D. V., Kahler, S. W., & Ng, C. K. 1997, ApJ, 491, 414
Roelof, E. C., Gold, R. E., Simnett, G. M., et al. 1992, GeoRL, 19, 1243
Schlickeiser, R. 2002, Cosmic Ray Astrophysics (Berlin: Springer)
Shalchi, A., Bieber, J. W., & Matthaeus, W. H. 2004, ApJ, 604, 675
Shalchi, A., Li, G., & Zank, G. P. 2010, Ap&SS, 325, 99
Skilling, J. 1971, ApJ, 170, 265
Tan, L. C., Reames, D. V., Ng, C. K., Saloniemi, O., & Wang, L. 2009, ApJ, 701, 1753
Teufel, A., & Schlickeriser, R. 2003, A&A, 397, 15
Wang, Y., Qin, G., & Zhang, M. 2012, ApJ, 752, 37
Wiedenbeck, M. E., Mason, G. M., Gómez-Herrero, R., et al. 2010, in AIP Conf. Proc. 1216, Twelfth International Solar Wind Conference, ed. M. Maksimovic, N. Meyer-Vernet, M. Moncuquet, & F. Pantellini (Melville, NY: AIP), 621
Zank, G. P., Li, G., Florinski, V., et al. 2004, JGR, 109, A04107
Zank, G. P., Rice, W. K. M., & Wu, C. C. 2000, JGR, 105, 25079
Zhang, M. 1999, ApJ, 513, 409
Zhang, M., Jokipii, J. R., & McKibben, R. B. 2003, ApJ, 595, 493
Zhang, M., Qin, G., & Rassoul, H. 2009, ApJ, 692, 109